Title

Growing Threats From Swings Between Hot and Wet Extremes in a Warmer World

Journal

Geophysical Research Letters, 50(14)

ISSN

0094-8276

Authors

You, Jiewen

Wang, Shuo

Zhang, Boen

et al.

Publication Date

2023-07-28

DOI

10.1029/2023gl104075

Growing Threats from Swings between Hot and Wet Extremes in a Warmer World

Jiewen You[1], Shuo Wang[1,*], Boen Zhang[1], Colin Raymond[2], Tom Matthews[3]

[1]Department of Land Surveying and Geo-Informatics and Research Institute for Land and Space, The Hong Kong Polytechnic University, Hong Kong, China

[2]Joint Institute for Regional Earth System Science and Engineering, University of California, Los Angeles, Los Angeles, CA, United States of America

[3]Department of Geography, Kings College London, London, UK

Corresponding author: Shuo Wang (shuo.s.wang@polyu.edu.hk)

Key Points

- Interactions between hot and wet extremes cause them to jointly occur about 15% more often than would be expected by chance.
- Increases in hot-wet compound events largely result from global-mean warming.
- Vapor-pressure-deficit anomalies are a signature of heat-pluvial versus pluvial-heat sequences, a conclusion enabled by field significance tests.

Abstract

The abrupt alternation between hot and wet extremes can lead to more severe societal impacts than isolated extremes. However, despite an understanding of hot and wet extremes separately, their temporally compounding characteristics are not well examined yet. Our study presents a comprehensive assessment of successive heat-pluvial and pluvial-heat events globally. We find that these successive extremes within a week occur every 6–7 years on average within warm seasons during 1956–2015, about 15% more often than would be expected by chance, and that they have a significant increase in frequency of about 22% per decade due to warming. We further investigate the role of vapor pressure deficit (VPD) and find that heat-pluvial (pluvial-heat) events are linked to negative (positive) VPD anomalies. Our results are statistically significant based on moving-blocks bootstrap resampling and field significance tests, highlighting these methods' importance in robustly identifying compound events under multiple-testing conditions.

Plain Language Summary

In recent years, the world has experienced various clustered weather and climate extremes, which are highly disruptive to humans and society. However, current knowledge on the risk of successive occurrence of hot (humid heat, including the effects of both temperature and humidity) and wet (pluvial flooding, usually caused by extreme rainfall) extremes remains unclear. In this study, we present a comprehensive assessment of the two types of interacting hot and wet extremes: humid heat extremes followed by pluvial flooding (heat-pluvial) and extreme pluvials followed by humid heat (pluvial-heat). We find that these events have increased significantly in most regions of the world for the last three decades, which can be associated with the warming effect. Importantly, we identify that the vapor pressure deficit plays an important but varying role in the abrupt alternation between heat and pluvial events. We emphasize the importance of using reliable statistical tests to ensure the validity of the results for complex compound events. Our analysis highlights the need for policymakers and stakeholders to develop adaptation strategies to cope with overlapping vulnerabilities due to compound hot and wet extremes, especially in areas prone to both such as West Australia, South America and Sub-Saharan Africa.

1. Introduction

Humid heat and pluvial flooding extremes have devastating impacts on humans, ecosystems, and society (Mora et al., 2017; Raymond, Matthews, et al., 2020; Tellman et al., 2021; UNDRR & CRED, 2020). Previous studies have typically considered one hazard (humid heat or pluvial flooding) and its impacts at a time. In recent years, a number of studies have investigated the spatiotemporal compounding of multiple extremes, defined as "compound events" (Bevacqua et al., 2021; Raymond, Horton, et al., 2020; Zscheischler et al., 2018, 2020). Compared to the well-established compound events that occur simultaneously such as concurrent droughts and heatwaves (Mukherjee & Mishra, 2021; Ridder et al., 2020), temporally compounding events that occur in close succession have yet to be well-understood, especially in the case of consecutive hot and wet extremes where the transition may be associated with convection and therefore difficult to forecast. This difficulty bears on the challenge of quantifying the causal link between extreme heat and nearby pluvial flooding, which seldom occur at precisely the same location and involve a range of atmosphere-ocean-land interactions at various scales.

A rapid transition from hot to wet conditions may occur because of large-scale processes related to the water cycle, atmospheric dynamics, and their feedbacks; in the subtropics and mid-latitudes, for example, this can include the movement of features such as areas of enhanced monsoon convection or the jet stream meandering (Shang et al., 2020; Shimpo et al., 2019; Swain et al., 2016; Z. Wang et al., 2019). There may also be direct linkages: high temperatures are a key factor contributing to atmospheric instability, potentially leading to or enhancing localized precipitation events that terminate previous heat events through strong evaporational cooling (Berg et al., 2013; Fowler et al., 2021; G. Wang et al., 2017). The other side of the coin is the occurrence of pluvials followed by heat events, which may be associated with tropical cyclone-released diabatic heating effects or region-scale thermal advection (Chen et al., 2021; Emanuel, 2003; Hart et al., 2007; Parker et al., 2013; Sukhovey & Camara, 1995). Another important physical mechanism is that the elevated moisture fluxing into the atmosphere during a pluvial event can increase atmospheric latent heat content, which may result in higher near-surface wet-bulb temperatures favourable for the occurrence of humid heat (X. Liu et al., 2017, 2019; Tom Matthews et al., 2022; Speizer et al., 2022).

When extreme heat is combined with pluvial flooding or vice versa in close succession, adverse impacts can be exacerbated due to the short recovery time. For successive heat-pluvial events, a sequence of heat extremes followed by pluvial flooding occurred in the United States in September 2017 (Cappucci, 2019), in the United Kingdom in August 2020 (ITV Weather, 2020) and in South Korea in July 2020 (Min et al., 2022), leading in each case to severe infrastructure damages, livestock deaths, and flood-related morbidity/mortality. The biggest threat is that people are generally not well prepared for high-intensity rainfall during prolonged hot weather; when it does occur, it can be so rapid that people have little time to adjust and safely evacuate (De Ruiter et al., 2020; T. Matthews et al., 2019; Raymond, Horton, et al., 2020). As an example of a successive pluvial-heat event, Japan experienced heavy rainfall and subsequent extreme heat in July 2018, causing more than 300 fatalities and large economic losses (Kawase et al., 2020; S. S. Y. Wang et al., 2019). The landfalls of tropical cyclones Irma and Ida in Florida and Louisiana, respectively, led to notable health impacts on residents who in the storms' aftermath were without air conditioning to combat the typical high heat stress values of late summer (Chatlani & Madden, 2021; Skarha et al., 2021). In such cases, the subsequent extreme heat adds to impacts in affected areas because the damage to infrastructure such as roads and power grids makes it more difficult to avoid heat exposure, and to obtain treatment in the case of heat illness (Issa et al., 2018). These recent examples highlight the importance of investigating the temporally compounding characteristics of heat-pluvial and pluvial-heat extremes more broadly.

Compared to well-understood underlying dependent drivers (e.g., concurrent drought and heatwave), quantifying the relationship between temporally compounding hot and wet extremes remains challenging. Recently, Zhang & Villarini (W. Zhang & Villarini, 2020) investigated compound heat stress and flooding events in the central United States and found that a high percentage of floods are preceded by a heat stress event. You & Wang (You & Wang, 2021) explored consecutive heat wave and heavy rainfall events in China and found that higher occurrence probability of hotter and shorter heat waves followed by heavy rainfall compared to heat waves not followed by heavy rainfall. Consecutive heat and pluvial events have also been investigated in previous studies, again focused on China (Chen et al., 2021; Liao et al., 2021). Globally, an increasing percentage of floods are likely to be accompanied by hot extremes, using observed dry bulb temperature for the identification of heat extremes and hydrological models for the simulation of flood hazards (Gu et al., 2022). Compared to dry heat, however, humid heat measures (that include the effects of both temperature and humidity) better capture the physiological drivers of heat stress and therefore are more likely to reflect dangerous conditions (Mora et al., 2017; Raymond et al., 2021). More importantly, the use of coarse-resolution general circulation models (GCMs) (~100–300 km) and simple hydrological models can lead to considerable uncertainty in projecting spatially resolved flood risks caused by heavy precipitation (Duethmann et al., 2020; Grimaldi et al., 2019; B. Zhang et al., 2021). Consequently, there is a need for thorough assessments of the spatiotemporal projections of temporally compounding heat and pluvial events, as well as descriptions of the underlying factors.

Here, we present a comprehensive global analysis of changes in the frequency of temporally compounding heat and pluvial events and their potential influencing factors. Temporally compounding humid heat extremes followed by pluvial extremes are referred to as heat-pluvial events; extreme pluvials followed by humid heat events are termed pluvial-heat events. We aim to gain a comprehensive understanding of global shifts between heat and pluvial events over the last sixty years by detecting compound events, conducting decomposition analysis, and identifying influential factors.

2. Methods

2.1. Datasets, regions, and seasons

In this study, we identify heat-pluvial and pluvial-heat events using two datasets: the 5th generation of ECMWF (The European Centre for Medium Range Weather Forecasts) global reanalysis (ERA5) (Hersbach et al., 2020) and National Centers for Environmental Prediction (NCEP) (Kalnay et al., 1996), respectively. These datasets include four essential variables (daily mean temperature, precipitation, specific humidity, and air pressure at 2m from the surface) with global coverage at the daily timescale. We use the ERA5 dataset for our main analysis, and test the sensitivity of our results with the alternative NCEP dataset. To avoid physical inconsistency among different data products, we identify events using variables from each dataset independently.

Our analysis spans 1956-2015 because it is the common period for ERA5 and NCEP. All datasets have been regridded to a common $2.5^{\circ} \times 2.5^{\circ}$ grid using the bilinear interpolation. We restrict the analysis to global land areas except for Greenland, Antarctica, and desert regions where annual precipitation is less than 100 mm. We only use data during local summer (May−September in the Northern Hemisphere, November−March in the Southern Hemisphere), as heat and pluvial events occur primarily in the warm season. As with previous global studies (Mukherjee & Mishra, 2021; Perkins-Kirkpatrick & Lewis, 2020), our selections of local summer seasons may miss some events in tropical regions where locally extreme heat may occur at almost any time of year.

2.2. Identification of successive heat and pluvial events, frequencies, and trends

We consider locally and seasonally varying thresholds when defining heat and pluvial events, with percentile values calculated from the entire 60-year period (1956–2015). A heat event includes the combined effect of high temperature and high humidity as characterized by the wet-bulb temperature (Buzan et al., 2015; Davies-Jones, 2008; Raymond, Matthews, et al., 2020), and is defined as a period when the daily wet-bulb temperature exceeds the 90th percentile for at least three consecutive days. The weighted average of precipitation is adopted to identify pluvial events (Lu, 2009). The index comprises day-of precipitation as well as the gradually diminishing impact of earlier precipitation by using a weighted average, where the weight declines proportionally with each passing day (Chen et al., 2021; Liao et al., 2021) (see details in Text S1). A pluvial event is defined as a period when the daily weighted average of precipitation exceeds the 90th percentile for at least three consecutive days.

Successive heat-pluvial and pluvial-heat events are heat events followed by pluvial events within a 7-day interval, and likewise for pluvial-heat events (see a sensitivity analysis of the time interval in Supporting Information). The 7-day interval was selected to balance the trade-off between potential impact and adequate sample size. We have also tested alternative time intervals, which are described in the Supplementary Information. To handle the occurrence of multiple heat events and pluvial events within a week, we cluster two successive heat or pluvial events into a single event if they are separated by two days or less.

We also calculate spatiotemporal changes in successive heat-pluvial and pluvial-heat events between the two 30-year periods (1986–2015 minus 1956–1985). To better compare the trends between different datasets, we use a normalized frequency ratio where the raw frequencies are first normalized by calculating annual values as a fraction of the 1956–2015 mean. The linear trend of annual values of successive heat-pluvial and pluvial-heat events is calculated using the Sen-slope method (unit, decade^{-1}) and the related significance is calculated using the Mann–Kendall test.

2.3. Moving-blocks bootstrap-resampling-based significance test

As the sequential occurrence of heat and pluvial events at a given location can be relatively rare and largely a matter of chance, traditional methods that estimate compound-event frequency based on event coincidence may struggle to identify causal relationships leading to successive extremes (Chen et al., 2021). To address this issue, we use a bootstrap resampling-based significance test to investigate the dependence of two time series, which can test whether the observations are significantly different from what would be expected due to chance alone. In practice, to consider autocorrelation when randomly sampling time series, the moving-blocks bootstrapping is utilized to perform the significance test (Vogel & Shallcross, 1996; Wilks, 1997) using a block size of three days. A sensitivity test using alternative block sizes (such as 5 or 10) did not change the significance of our findings. We implemented the moving-blocks bootstrap-resampling-based significance test for each gridcell in the following steps: (1) Identify the heat and pluvial event series from 1956 to 2015; (2) Generate 1,000 resampled event series using the moving-blocks bootstrap, where each resampled series has the same length as the original series. By randomly permuting the event series, rather than the original daily time series, all relevant statistical attributes can be preserved; (3) Compute the occurrence frequencies of heat-pluvial and pluvial-heat events for each pair of resampled series using a pre-determined method (Section 2.2); (4) Compute the empirical distribution of consecutive occurrence frequencies using the 1,000 resampled series; (5) Compute the 95% confidence intervals of the empirical distribution of consecutive occurrence frequencies. (6) Compute the occurrence frequency of heat-pluvial and pluvial-heat events for the original series based on ERA5 and NECP datasets. (7) Determine whether the occurrence frequency of heat-pluvial and pluvial-heat events for the original series falls within the 95% confidence interval of the empirical distribution of consecutive occurrence frequencies; (8) If the occurrence frequency of heat-pluvial and pluvial-heat events for the original series is outside the 95% confidence interval, then it is statistically significant at the 0.05 level.

2.4. Decomposition of warming/moistening effects

In order to investigate the effects of warming and moistening on the change in temporally compounding heat and pluvial events between the two 30-year periods (recent, 1986–2015 minus past, 1956–1985), we calculate non-stationary 90th percentiles in time to re-define compound events and isolate the warming/moistening effects. In other words, we calculate and compare the difference in frequency of heat-pluvial or pluvial-heat between the two periods in each grid, with each calculation using events defined according to its native 30-year percentile, which allows for the percentile to change within the respective periods. Practically, to account for the warming effect only (i.e., removing the trend of weighted average of precipitation), we identify heat-pluvial events during 1956–1985 using the 1956–1985 weighted average of precipitation and likewise for 1986–2015, always keeping the wet-bulb temperature percentile constant in time. Similarly, to explore the moistening effect (i.e., removing the trend of wet-bulb temperature), we allow for the wet-bulb temperature percentile to change within the respective periods but hold the weighted average of precipitation percentile unchanged.

2.5. Investigation of VPD anomalies and field significance test

We investigate the potential impact of atmospheric humidity, measured by vapor pressure deficit (VPD), on the abrupt alternation between heat and pluvial events. For successive pluvial-heat events, we analyze the differences in VPD anomalies between heat events followed by pluvial events (i.e., heat-pluvial) and those not followed by pluvial events (i.e., heat-without-pluvial), specifically focusing on VPD conditions one day after the end of heat events. Similarly, for pluvial-heat events, we examine the differences in 1-day VPD anomalies between pluvial events followed by heat events (i.e., pluvial-heat) and those not followed by heat events (i.e., pluvial-without-heat).

To determine whether the observed differences in VPD are statistically significant and not solely due to chance, we conduct field significance tests to address the issue of multiple hypotheses (Wilks, 2006, 2016). Specifically, we control the false discovery rate (FDR) during these tests to minimize the likelihood of identifying false positive results (type I errors) when multiple tests are performed simultaneously. The FDR represents the proportion of rejected null hypotheses that are true. By controlling the FDR, we can increase confidence in the significance of our findings (Benjamini & Hochberg, 1995; Ventura et al., 2004; Wilks, 2006).

Practically, our analysis involves testing the global null hypothesis (H_0), which assumes no statistically significant differences in VPD between heat-pluvial and heat-without-pluvial events. To address the multi-hypothesis issue, we perform field significance tests by controlling FDR rates at a certain level q. This involves rejecting local null hypotheses whose p-values are no greater than a threshold p_{FDR}.

$$p_{\text{FDR}} = \max_{j=1,\ldots,\text{K}} [p_{(j)}: p_{(j)} \leq \alpha_0 \left(\frac{j}{N}\right)]$$

where N is the total number of local tests (i.e., grid points) and α_0 is the desired level of significance (0.05). To determine the largest K satisfying the equation, we need to order the p-values; any local tests with p-values smaller than or equal to the largest p-value are deemed to be field-significant (Wilks, 2006).

3. Results

3.1. Global climatology of heat-pluvial and pluvial-heat events

Using two independent reanalysis datasets (ERA5 and NCEP), we quantify the global frequency of successive heat-pluvial and pluvial-heat events during 1956–2015. As shown in Figure 1, successive heat-pluvial events have occurred for almost all global land (with desert and polar regions excluded as noted in Section 2.1). The total number of successive heat-pluvial events observed in the two datasets is about 11 on average during 1956–2015 for each gridcell. Successive pluvial-heat events occur slightly less frequently, with an average of approximately 10 over the 60-year study period. Furthermore, the significance of the detected successive events is confirmed using the moving-blocks bootstrap resampling-based significance test (Figures 1c and 1d). The test shows that the number of detected events based on both ERA5 and NCEP datasets exceed the 95% confidence interval estimates from moving-blocks bootstrap resampling that occur by chance, corresponding to the frequency of heat-pluvial and pluvial-heat of 9.74 and 8.48, respectively. This indicates that, on average globally, successive heat-pluvial events occur about 13-18% more often than would be expected by chance, likely a signature of correlated heat and precipitation via local thermodynamics (i.e. convection) or colliding contrasting air masses (i.e. weather fronts) (Liao et al., 2021; Shang et al., 2020).

Looking at the spatial distribution of the number of events, both successive heat-pluvial and pluvial-heat exhibit clear regional differences globally, as illustrated in Figure 1b. Such temporally compounding extremes occur most often in West Australia, East North America, Sub-Saharan Africa, and North Asia (Figure S2), where they are statistically significant at the 0.05 level according to the moving-blocks bootstrap-resampling-based test (Figure 1a). Compared to the successive heat-pluvial events, the pluvial-heat events occur less frequently, but some hotspots maintain consistency — such as West Australia (Figure 1b). The spatial patterns remain similar even when events are defined using a more extreme percentile, despite having reduced peaks (Figure S3).

3.2. Spatiotemporal changes in successive events and warming effect

We investigate the spatiotemporal changes in the frequency of temporally compounding heat and pluvial events from 1956 to 2015, by comparing the first (1956–1985) and second (1986–2015) 30-year periods, as shown in Figure 2a and Figures S5–S6. In most regions, a higher frequency of successive heat-pluvial events is observed in the later (1986–2015) period compared to the earlier window (1956–1985). A rising trend in event frequency is identified in most parts of South America, Sub-Saharan Africa, South Asia, and North Australia, with 15 or more events during the latest 30-year period. In general, the spatial patterns and temporal trends of ERA5 and NCEP are in good agreement (Figures S5–S6). However, there are some noticeable discrepancies over the eastern United States and sub-Saharan Africa, which may be attributed to a complex relationship between heat and convection, potentially related to statistical effects from sequential events. The overall frequency of temporally compounding heat and pluvial events has seen a statistically significant (Mann–Kendall test, $p < 0.05$) increase for both event subcategories, with an increase of about 20-25% per decade (Figures 2b, S6).

To explore further how the increases in individual extremes contribute to successive heat and pluvial events, we analyze the relationship between the changes in compound events and changes in individual extremes at the grid level between the two 30-year periods (Figure 2c, Figures S7–S8). In general, the upward trend in heat-pluvial event frequency is an expected consequence of these upward trends in univariate hazard frequencies. Specifically, our findings indicate that more areas experienced an increased frequency of individual heat events and compound heat-pluvial events, than of individual pluvial events and compound heat-pluvial events. This suggests that an increase in individual heat events is a more significant factor contributing to the rise in successive heat-pluvial events (Figure S9), and is consistent with our findings for successive pluvial-heat events (Figure S5–S9), as well as with other work suggesting that increases in heat dominate the trends in many compound events involving temperature and another variable (Gu et al., 2022; M. Liu et al., 2022; Yin et al., 2022).

To explain the increased trend of successive heat and pluvial events, we conduct a contribution decomposition analysis to disentangle the relative importance of the effects of warming and moistening on the trends of successive heat and pluvial events (Figure 2d and Figure S10). We examine the change of trends by constructing four realizations of time series: (1) with warming and moistening (original observational data); (2) without warming and moistening (remove trends of wet-bulb temperature and weighted average of precipitation); (3) warming alone (remove the trend of weighted average of precipitation) and (4) moistening alone (remove the trend of wet-bulb temperature). We find that for heat-pluvial or pluvial-heat events, the effect of warming alone can reproduce the observed trends (Figure 3a). The effect of warming is especially prominent in South America, South Asia, and North Australia, which are co-located with hotspots in Figure 2a, while moistening without warming has little effect (Figures S10–S11). In other words, once the warming effect has been removed there is no 'residual' increase in successive events. Therefore, it is the increased heat extremes under a warming climate that have made successive heat-pluvial and pluvial-heat events occur more frequently in recent decades.

3.3. Possible factor affecting the transitions between heat and pluvial events

In this section, we further examine the influence of VPD on transitions between heat and pluvial events. To address the issue of multiple hypothesis testing resulting from spatial dependence, we have conduct a field significance test to determine whether the differences in VPD between heat-pluvial and heat-without-pluvial events are statistically significant or not (Section 2.5). We find significant differences in VPD exist between heat-pluvial and heat-without-pluvial events for about 85% of gridcells at the p=0.05 level (Figure 3), as well as a similar number for the comparison between pluvial-heat and heat-without-pluvial events using FDR test (Figure S12). Importantly, we reveal that small and negative VPD anomalies are linked to the transition from heat to pluvial (Figures 3a and c), while high positive VPD anomalies accompany the transition from pluvial to heat (Figures 3b and c). This can be explained by the increased water supply due to subsequent pluvial and reduced heating at the end of heat events, which may be associated with reduced VPD through transpiration from plants (Massmann et al., 2019; Yuan et al., 2019). Low VPD can alleviate some of the effects of extreme temperatures on plant health (Grossiord et al., 2020; Novick et al., 2016), and the high moisture content can supply the fuel for pluvial events, especially of a convective nature. On the contrary, increased VPD anomalies imply high atmospheric aridity, related to the termination of pluvial events and the abrupt onset of heat events. This finding echoes the observational evidence that high VPD enhances atmospheric demand for water, depleting soil moisture and simultaneously heating the atmospheric boundary layer (Teuling et al., 2013; Zhou et al., 2019).

4. Discussions and Conclusions

Humid heat and pluvial flooding are serious weather extremes by themselves, but when occurring sequentially at the same location, they can cause more severe consequences than an isolated extreme event. While extreme heat or pluvial flooding alone has attracted considerable attention over the past decades (Fischer et al., 2021; Martin, 2018; Sun et al., 2021; P. Wang et al., 2021), the global climatology of successive heat and pluvial events remains unclear. In this study, we perform a comprehensive global assessment of heat-pluvial and pluvial-heat events. Based on two datasets, we reveal the baseline frequencies and spatiotemporal changes of successive extremes. Our findings demonstrate the increased risk of rapid transition between heat and pluvial events in a warmer climate in recent decades. Hotspots are centered in West Australia, East North America, Sub-Saharan Africa, and North Asia. We find that more frequent heat extremes due to a warming climate have resulted in a higher incidence of heat-pluvial and pluvial-heat events. Furthermore, our findings demonstrate that notable VPD anomalies are typically observed in association.

To ensure the consistency and robustness of the analysis, we conduct multiple sensitivity analyses related to data sources, time intervals and thresholds, and alternative event definition (see details in Text S2). Although the frequency of successive heat-pluvial and pluvial-heat events is very sensitive to the choice of event definitions, extreme thresholds and time lags (Figures S13–S18), our main results of increased trends in successive heat-pluvial and pluvial-heat events are robust (Figures S13–S14). Disagreement between datasets has the largest effect on our results for eastern United States and sub-Saharan Africa regions.

Extreme temporally compound events are often rare, and their occurrence can be coincidental due to chance. Our study highlights the value of using bootstrapping resampling-based significance tests, a method that has been overlooked in previous studies (Chen et al., 2021; W. Zhang & Villarini, 2020). Specifically, it is important to consider autocorrelation when randomly sampling time series of rainfall and temperature, particularly for event definitions based on individual hot and wet days with no duration requirement. The moving-blocks bootstrapping method used in this study accounts for the uncertainty in temporally correlated event coincidence by generating a set of surrogate time series that have the same statistical properties, including temporal structure, as the original time series (Vogel & Shallcross, 1996).

We also show VPD has crucial but different impacts on successive heat-pluvial and pluvial-heat events, respectively. Small and negative VPD anomalies are linked to successive heat-pluvial events, while successive occurrences of pluvial-heat events are more likely to exhibit a positive VPD anomaly. We confirm that observed differences in VPD are not due to random chance or measurement error, but rather reflect real differences between the two types of events based on field significance test. To ensure the robustness of our analysis, we also use two alternative methods: Walker's test and moving block bootstrapping-based multivariate test, both of which provide consistent results (see details in Text S3, Figures S19–S22). Our findings underscore the importance of using field significance tests to determine the statistical significance of observed differences or relationships, particularly for data with spatial dependence (Wilks, 2016; Zscheischler & Seneviratne, 2017). In our study, we find that while 1293 grid elements achieved local statistical significance at the 0.05 level, 1282 grid elements have p-values that meet the FRD criterion, indicating statistically field significance. Although the difference is small, the latter approach using field significance tests provides a more accurate and reliable statistical significance assessment and helps prevent overestimating results. These findings have important implications when dealing with climate data and other datasets with spatial dependence, highlighting the need to use field significance tests to evaluate the significance of findings and avoid overestimating the significance.

Overall, our study indicates that VPD plays a vital role in temporally compounding heat and pluvial events, which are often ignored in previous compound events. Importantly, we highlight the asymmetric impacts of VPD on the rapid transitions between heat and pluvial extremes, which could provide a reference and insight into early warning and anticipation of emerging temporally compounding hydrological hazards. The physical mechanisms underlying compound heat and pluvial events are complex. While detecting and presenting a global assessment of two emerging compound extremes was our priority and focus in this study, identifying the process-based evolution and underlying mechanisms of the rapid transition from extreme heat to pluvial or vice versa from a physical standpoint is an important and challenging task. Future studies should be undertaken to further investigate these mechanisms and help advance our understanding of compound hazards.

Open Research

All data in this study are publicly available. The daily gridded daily mean temperature, precipitation, specific humidity, and air pressure are provided by European Centre for Medium-Range Weather Forecasts Reanalysis 5 (ERA5, https://cds.climate.copernicus.eu/cdsapp#!/dataset/reanalysis-era5-single-levels), and National Centers for Environmental Prediction (NCEP, https://psl.noaa.gov/data/gridded/data.ncep.reanalysis.html).

Acknowledgments

This research was supported by the Hong Kong Research Grants Council Early Career Scheme (Grant No. 25222319) and the Hong Kong Research Grants Council Ph.D. Fellowship Scheme (Grant No. PF19-35676). A portion of this work was carried out at the Jet Propulsion

Laboratory, California Institute of Technology, under a contract with the National Aeronautics and Space Administration (80NM0018D0004).

References

Benjamini, Y., & Hochberg, Y. (1995). Controlling the false discovery rate: a practical and powerful approach to multiple testing. *Journal of the Royal Statistical Society: Series B (Methodological)*, *57*(1), 289–300. https://doi.org/10.1111/j.2517-6161.1995.tb02031.x

Berg, P., Moseley, C., & Haerter, J. O. (2013). Strong increase in convective precipitation in response to higher temperatures. *Nature Geoscience*, *6*(3), 181–185. https://doi.org/10.1038/ngeo1731

Bevacqua, E., De Michele, C., Manning, C., Couasnon, A., Ribeiro, A. F. S., Ramos, A. M., et al. (2021). Guidelines for studying diverse types of compound weather and climate events. *Earth's Future*, *9*(11), e2021EF002340. https://doi.org/10.1029/2021EF002340

Buzan, J. R., Oleson, K., & Huber, M. (2015). Implementation and comparison of a suite of heat stress metrics within the Community Land Model version 4.5. *Geoscientific Model Development*, *8*(2), 151–170. https://doi.org/10.5194/gmd-8-151-2015

Cappucci, M. (2019). Storms deluge New York city, abruptly ending sweltering heat wave, available at: https://www.washingtonpost.com/weather/2019/07/23/flooding-rain-deluges-new-york-city-abruptly-ending-sweltering-heat-wave/, last access: 25 April 2022.

Chatlani, S., & Madden, P. (2021). 9 dead from excessive heat in New Orleans in wake of Hurricane Ida. Retrieved May 26, 2022, from https://www.wwno.org/news/2021-09-08/11-dead-from-excessive-heat-in-new-orleans-in-wake-of-hurricane-ida

Chen, Y., Liao, Z., Shi, Y., Tian, Y., & Zhai, P. (2021). Detectable increases in sequential flood-heatwave events across China during 1961–2018. *Geophysical Research Letters*, *48*(6), e2021GL092549. https://doi.org/10.1029/2021GL092549

Davies-Jones, R. (2008). An efficient and accurate method for computing the wet-bulb temperature along pseudoadiabats. *Monthly Weather Review*, *136*(7), 2764–2785. https://doi.org/10.1175/2007MWR2224.1

De Ruiter, M. C., Couasnon, A., Homberg, M. J. C., Daniell, J. E., Gill, J. C., & Ward, P. J. (2020). Why we can no longer ignore consecutive disasters. *Earth's Future*, *8*(3). https://doi.org/10.1029/2019EF001425

Duethmann, D., Blöschl, G., & Parajka, J. (2020). Why does a conceptual hydrological model fail to correctly predict discharge changes in response to climate change? *Hydrology and Earth System Sciences*, *24*(7), 3493–3511. https://doi.org/10.5194/hess-24-3493-2020

Emanuel, K. (2003). Tropical Cyclones. *Annual Review of Earth and Planetary Sciences*, *31*(1), 75–104. https://doi.org/10.1146/annurev.earth.31.100901.141259

Fischer, E. M., Sippel, S., & Knutti, R. (2021). Increasing probability of record-shattering climate extremes. *Nature Climate Change*, 1–7. https://doi.org/10.1038/s41558-021-01092-9

Fowler, H. J., Lenderink, G., Prein, A. F., Westra, S., Allan, R. P., Ban, N., et al. (2021). Anthropogenic intensification of short-duration rainfall extremes. *Nature Reviews Earth & Environment*, 1–16. https://doi.org/10.1038/s43017-020-00128-6

Grimaldi, S., Schumann, G. J.-P., Shokri, A., Walker, J. P., & Pauwels, V. R. N. (2019). Challenges, opportunities, and pitfalls for global coupled hydrologic-hydraulic modeling of floods. *Water Resources Research*, *55*(7), 5277–5300. https://doi.org/10.1029/2018WR024289

Grossiord, C., Buckley, T. N., Cernusak, L. A., Novick, K. A., Poulter, B., Siegwolf, R. T. W., et al. (2020). Plant responses to rising vapor pressure deficit. *New Phytologist*, *226*(6), 1550–1566. https://doi.org/10.1111/nph.16485

Gu, L., Chen, J., Yin, J., Slater, L. J., Wang, H.-M., Guo, Q., et al. (2022). Global increases in compound flood-hot extreme hazards under climate warming. *Geophysical Research Letters*, *49*(8), e2022GL097726. https://doi.org/10.1029/2022GL097726

Hart, R. E., Maue, R. N., & Watson, M. C. (2007). Estimating local memory of tropical cyclones through MPI anomaly evolution. *Monthly Weather Review*, *135*(12), 3990–4005. https://doi.org/10.1175/2007MWR2038.1

Hersbach, H., Bell, B., Berrisford, P., Hirahara, S., Horányi, A., Muñoz-Sabater, J., et al. (2020). The ERA5 global reanalysis. *Quarterly Journal of the Royal Meteorological Society*, *146*(730), 1999–2049. https://doi.org/10.1002/qj.3803

Issa, A., Ramadugu, K., Mulay, P., Hamilton, J., Siegel, V., Harrison, C., et al. (2018). Deaths related to Hurricane Irma — Florida, Georgia, and North Carolina, September 4–October 10, 2017. *MMWR. Morbidity and Mortality Weekly Report*, *67*(30), 829–832. https://doi.org/10.15585/mmwr.mm6730a5

ITV Weather. (2020). Two months' rain could fall in three hours as heatwave triggers thunderstorms, available at: https://www.itv.com/news/2020-08-10/two-months-rain-could-fall-in-three-hours-as-heatwave-triggers-thunderstorms, last access: 25 April 2022.

Kalnay, E., Kanamitsu, M., Kistler, R., Collins, W., Deaven, D., Gandin, L., et al. (1996). The NCEP/NCAR 40-Year Reanalysis Project. *Bulletin of the American Meteorological Society*, *77*(3), 437–472. https://doi.org/10.1175/1520-0477(1996)077<0437:TNYRP>2.0.CO;2

Kawase, H., Imada, Y., Tsuguti, H., Nakaegawa, T., Seino, N., Murata, A., & Takayabu, I. (2020). The heavy rain event of July 2018 in Japan enhanced by historical warming. *Bulletin of the*

American Meteorological Society, *101*(1), S109–S114. https://doi.org/10.1175/BAMS-D-19-0173.1

Liao, Z., Chen, Y., Li, W., & Zhai, P. (2021). Growing threats from unprecedented sequential flood-hot extremes across China. *Geophysical Research Letters*, *48*(18), e2021GL094505. https://doi.org/10.1029/2021GL094505

Liu, M., Yin, Y., Wang, X., Ma, X., Chen, Y., & Chen, W. (2022). More frequent, long-lasting, extreme and postponed compound drought and hot events in eastern China. *Journal of Hydrology*, *614*, 128499. https://doi.org/10.1016/j.jhydrol.2022.128499

Liu, X., Tang, Q., Zhang, X., Groisman, P., Sun, S., Lu, H., & Li, Z. (2017). Spatially distinct effects of preceding precipitation on heat stress over eastern China. *Environmental Research Letters*, *12*(11), 115010. https://doi.org/10.1088/1748-9326/aa88f8

Liu, X., Tang, Q., Liu, W., Yang, H., Groisman, P., Leng, G., et al. (2019). The asymmetric impact of abundant preceding rainfall on heat stress in low latitudes. *Environmental Research Letters*, *14*(4), 044010. https://doi.org/10.1088/1748-9326/ab018a

Lu, E. (2009). Determining the start, duration, and strength of flood and drought with daily precipitation: Rationale. *Geophysical Research Letters*, *36*(12). https://doi.org/10.1029/2009GL038817

Martin, E. R. (2018). Future projections of global pluvial and drought event characteristics. *Geophysical Research Letters*, *45*(21), 11,913-11,920. https://doi.org/10.1029/2018GL079807

Massmann, A., Gentine, P., & Lin, C. (2019). When Does Vapor Pressure Deficit Drive or Reduce Evapotranspiration? *Journal of Advances in Modeling Earth Systems*, *11*(10), 3305–3320. https://doi.org/10.1029/2019MS001790

Matthews, T., Wilby, R. L., & Murphy, C. (2019). An emerging tropical cyclone–deadly heat compound hazard. *Nature Climate Change*, *9*(8), 602–606. https://doi.org/10.1038/s41558-019-0525-6

Matthews, T., Byrne, M., Horton, R., Murphy, C., Pielke Sr, R., Raymond, C., et al. (2022). Latent heat must be visible in climate communications. *WIREs Climate Change*, e779. https://doi.org/10.1002/wcc.779

Min, S.-K., Jo, S.-Y., Seong, M.-G., Kim, Y.-H., Son, S.-W., Byun, Y.-H., et al. (2022). Human contribution to the 2020 summer successive hot-wet extremes in South Korea. *Bulletin of the American Meteorological Society*, 8. https://doi.org/10.1175/BAMS-D-21-0144.1

Mora, C., Dousset, B., Caldwell, I. R., Powell, F. E., Geronimo, R. C., Bielecki, C. R., et al. (2017). Global risk of deadly heat. *Nature Climate Change*, *7*(7), 501–506. https://doi.org/10.1038/nclimate3322

Mukherjee, S., & Mishra, A. K. (2021). Increase in compound drought and heatwaves in a warming world. *Geophysical Research Letters*, *48*(1), e2020GL090617. https://doi.org/10.1029/2020GL090617

Novick, K. A., Ficklin, D. L., Stoy, P. C., Williams, C. A., Bohrer, G., Oishi, A. C., et al. (2016). The increasing importance of atmospheric demand for ecosystem water and carbon fluxes. *Nature Climate Change*, *6*(11), 1023–1027. https://doi.org/10.1038/nclimate3114

Parker, T. J., Berry, G. J., & Reeder, M. J. (2013). The influence of tropical cyclones on heat waves in Southeastern Australia. *Geophysical Research Letters*, *40*(23), 6264–6270. https://doi.org/10.1002/2013GL058257

Perkins-Kirkpatrick, S. E., & Lewis, S. C. (2020). Increasing trends in regional heatwaves. *Nature Communications*, *11*(1), 3357. https://doi.org/10.1038/s41467-020-16970-7

Raymond, C., Matthews, T., & Horton, R. M. (2020). The emergence of heat and humidity too severe for human tolerance. *Science Advances*, *6*(19), eaaw1838. https://doi.org/10.1126/sciadv.aaw1838

Raymond, C., Horton, R. M., Zscheischler, J., Martius, O., AghaKouchak, A., Balch, J., et al. (2020). Understanding and managing connected extreme events. *Nature Climate Change*, *10*(7), 611–621. https://doi.org/10.1038/s41558-020-0790-4

Raymond, C., Matthews, T., Horton, R. M., Fischer, E. M., Fueglistaler, S., Ivanovich, C., et al. (2021). On the controlling factors for globally extreme humid heat. *Geophysical Research Letters*, *48*(23), e2021GL096082. https://doi.org/10.1029/2021GL096082

Ridder, N. N., Pitman, A. J., Westra, S., Ukkola, A., Hong, X. D., Bador, M., et al. (2020). Global hotspots for the occurrence of compound events. *Nature Communications*, *11*(1), 5956. https://doi.org/10.1038/s41467-020-19639-3

Shang, W., Ren, X., Duan, K., & Zhao, C. (2020). Influence of the South Asian high-intensity variability on the persistent heavy rainfall and heat waves in Asian monsoon regions. *International Journal of Climatology*, *40*(4), 2153–2172. https://doi.org/10.1002/joc.6324

Shimpo, A., Takemura, K., Wakamatsu, S., Togawa, H., Mochizuki, Y., Takekawa, M., et al. (2019). Primary factors behind the heavy rain event of July 2018 and the subsequent heat wave in Japan. *Sola*, *advpub*. https://doi.org/10.2151/sola.15A-003

Skarha, J., Gordon, L., Sakib, N., June, J., Jester, D. J., Peterson, L. J., et al. (2021). Association of power outage with mortality and hospitalizations among Florida nursing home residents after hurricane Irma. *JAMA Health Forum*, *2*(11), e213900. https://doi.org/10.1001/jamahealthforum.2021.3900

Speizer, S., Raymond, C., Ivanovich, C., & Horton, R. M. (2022). Concentrated and intensifying humid heat extremes in the IPCC AR6 Regions. *Geophysical Research Letters*, *49*(5), e2021GL097261. https://doi.org/10.1029/2021GL097261

Sukhovey, V. F., & Camara, T. (1995). Thermal advection in the tropical Atlantic upper layer. *Physical Oceanography*, *6*(6), 399–410. https://doi.org/10.1007/BF02197465

Sun, Q., Zhang, X., Zwiers, F., Westra, S., & Alexander, L. V. (2021). A global, continental, and regional analysis of changes in extreme precipitation. *Journal of Climate*, *34*(1), 243–258. https://doi.org/10.1175/JCLI-D-19-0892.1

Swain, D. L., Horton, D. E., Singh, D., & Diffenbaugh, N. S. (2016). Trends in atmospheric patterns conducive to seasonal precipitation and temperature extremes in California. *Science Advances*, *2*(4), e1501344. https://doi.org/10.1126/sciadv.1501344

Tellman, B., Sullivan, J. A., Kuhn, C., Kettner, A. J., Doyle, C. S., Brakenridge, G. R., et al. (2021). Satellite imaging reveals increased proportion of population exposed to floods. *Nature*, *596*(7870), 80–86. https://doi.org/10.1038/s41586-021-03695-w

Teuling, A. J., Van Loon, A. F., Seneviratne, S. I., Lehner, I., Aubinet, M., Heinesch, B., et al. (2013). Evapotranspiration amplifies European summer drought. *Geophysical Research Letters*, *40*(10), 2071–2075. https://doi.org/10.1002/grl.50495

UNDRR, & CRED. (2020). Human cost of disasters: An overview of the last 20 years, 2000-2019. *UN Office for Disaster Risk Reduction (UNDRR), Centre for Research on the Epidemiology of Disaster (CRED)*.

Ventura, V., Paciorek, C. J., & Risbey, J. S. (2004). Controlling the proportion of falsely rejected hypotheses when conducting multiple tests with climatological data. *Journal of Climate*, *17*(22), 4343–4356. https://doi.org/10.1175/3199.1

Vogel, R. M., & Shallcross, A. L. (1996). The moving blocks bootstrap versus parametric time series models. *Water Resources Research*, *32*(6), 1875–1882. https://doi.org/10.1029/96WR00928

Wang, G., Wang, D., Trenberth, K. E., Erfanian, A., Yu, M., Bosilovich, M. G., & Parr, D. T. (2017). The peak structure and future changes of the relationships between extreme precipitation and temperature. *Nature Climate Change*, *7*(4), 268–274. https://doi.org/10.1038/nclimate3239

Wang, P., Yang, Y., Tang, J., Leung, L. R., & Liao, H. (2021). Intensified humid heat events under global warming. *Geophysical Research Letters*, *48*(2), e2020GL091462. https://doi.org/10.1029/2020GL091462

Wang, S. S. Y., Kim, H., Coumou, D., Yoon, J.-H., Zhao, L., & Gillies, R. R. (2019). Consecutive extreme flooding and heat wave in Japan: Are they becoming a norm? *Atmospheric Science Letters*, *20*(10), e933. https://doi.org/10.1002/asl.933

Wang, Z., Yang, S., Duan, A., Hua, W., Ullah, K., & Liu, S. (2019). Tibetan Plateau heating as a driver of monsoon rainfall variability in Pakistan. *Climate Dynamics*, *52*(9), 6121–6130. https://doi.org/10.1007/s00382-018-4507-6

Wilks, D. S. (1997). Resampling hypothesis tests for autocorrelated fields. *Journal of Climate*, *10*(1), 65–82. https://doi.org/10.1175/1520-0442(1997)010<0065:RHTFAF>2.0.CO;2

Wilks, D. S. (2006). On “field significance” and the false discovery rate. *Journal of Applied Meteorology and Climatology*, *45*(9), 1181–1189. https://doi.org/10.1175/JAM2404.1

Wilks, D. S. (2016). “The stippling shows statistically significant grid points”: how research results are routinely overstated and overinterpreted, and what to do about it. *Bulletin of the*

American Meteorological Society, *97*(12), 2263–2273. https://doi.org/10.1175/BAMS-D-15-00267.1

Yin, J., Slater, L., Gu, L., Liao, Z., Guo, S., & Gentine, P. (2022). Global increases in lethal compound heat stress: hydrological drought hazards under cimate change. *Geophysical Research Letters*, *49*(18), e2022GL100880. https://doi.org/10.1029/2022GL100880

You, J., & Wang, S. (2021). Higher probability of occurrence of hotter and shorter heat waves followed by heavy rainfall. *Geophysical Research Letters*, *48*(17), e2021GL094831. https://doi.org/10.1029/2021GL094831

Yuan, W., Zheng, Y., Piao, S., Ciais, P., Lombardozzi, D., Wang, Y., et al. (2019). Increased atmospheric vapor pressure deficit reduces global vegetation growth. *Science Advances*, *5*(8), eaax1396. https://doi.org/10.1126/sciadv.aax1396

Zhang, B., Wang, S., & Wang, Y. (2021). Probabilistic projections of multidimensional flood risks at a convection-permitting scale. *Water Resources Research*, *57*(1), e2020WR028582. https://doi.org/10.1029/2020WR028582

Zhang, W., & Villarini, G. (2020). Deadly compound heat stress-flooding hazard across the central United States. *Geophysical Research Letters*, *47*(15), e2020GL089185. https://doi.org/10.1029/2020GL089185

Zhou, S., Williams, A. P., Berg, A. M., Cook, B. I., Zhang, Y., Hagemann, S., et al. (2019). Land–atmosphere feedbacks exacerbate concurrent soil drought and atmospheric aridity. *Proceedings of the National Academy of Sciences*, *116*(38), 18848–18853. https://doi.org/10.1073/pnas.1904955116

Zscheischler, J., & Seneviratne, S. I. (2017). Dependence of drivers affects risks associated with compound events. *Science Advances*, *3*(6), e1700263. https://doi.org/10.1126/sciadv.1700263

Zscheischler, J., Westra, S., van den Hurk, B. J. J. M., Seneviratne, S. I., Ward, P. J., Pitman, A., et al. (2018). Future climate risk from compound events. *Nature Climate Change*, *8*(6), 469–477. https://doi.org/10.1038/s41558-018-0156-3

Zscheischler, J., Martius, O., Westra, S., Bevacqua, E., Raymond, C., Horton, R. M., et al. (2020). A typology of compound weather and climate events. *Nature Reviews Earth & Environment*, *1*(7), 333–347. https://doi.org/10.1038/s43017-020-0060-z

List of Figure Captions

Figure 1. Frequency of successive heat-pluvial and pluvial-heat events within 7 days during 1956–2015. a, b Spatial maps showing the total number of successive heat-pluvial and pluvial-heat events, respectively. Gridcells that are statistically significant at the 0.05 level according to the moving-blocks bootstrap-resampling-based test are depicted as grey circles. The dataset used here is ERA5. **c, d** Significance test of the global-mean consecutive occurrence frequencies using moving-blocks bootstrap resampling based on ERA5 dataset for the heat-pluvial events (**c**) and pluvial heat events (**d**), respectively. The histogram represents the empirical distribution of successive events frequency using the 1,000 resampled series based on the moving-blocks bootstrap resampling. The 95% confidence interval is indicated by a vertical dashed line. The red dot and blue dot represent the number of successive events detected based on ERA5 and NCEP datasets, respectively.

Figure 2. Spatiotemporal changes and decomposition in the frequency of successive heat-pluvial events within 7 days. a Spatial change in successive heat-pluvial events between the two 30-year periods (recent, 1986–2015 minus past, 1956–1985). **b** Annual time series of the normalized frequency ratio of successive heat-pluvial events. Black line is the annual normalized frequency ratio based on ERA5; blue dashed line is the 30-year average. dRatio is the difference between the averages during 1956–1985 and 1986–2015; Slope is the linear trend using the Sen-slope method (unit, decade-1). **c** The relationship between the changes in successive events and changes in individual extremes. Color circles show bin-averaged ratios of heat-pluvial events corresponding to ratios of individual extremes. **d** Decomposition of the frequency of heat-pluvial events due to warming/moistening effects. It shows the probability density function of the global

mean changes in the frequency of heat-pluvial events between the two 30-year periods, based on raw observational data (black), data with moistening signal removed (red), data with warming signal removed (blue) and data with both warming and moistening signals removed (green).

Figure 3. The behavior of VPD anomalies in the transition between heat and pluvial events. **a** represents VPD anomalies between heat events followed by pluvial events (heat-pluvial) and heat events not followed by pluvial events (heat-without-pluvial). **b** represents VPD anomalies between pluvial events followed by heat events (pluvial-heat) and pluvial events not followed by heat events (pluvial-without-heat). Grid points that satisfy local statistical significance at the 0.05 level are shown as grey circles, while the ones that meet the FDR criterion by having a sufficiently small p-value are marked by grey points. **c** is the probability density function of the map **a** (green line) and **b** (red line) for the VPD anomalies causing the transition between heat and pluvial events. **d** is the FDR for testing field significance of VPD anomalies (Pa) between heat-pluvial and heat-without-pluvial events.

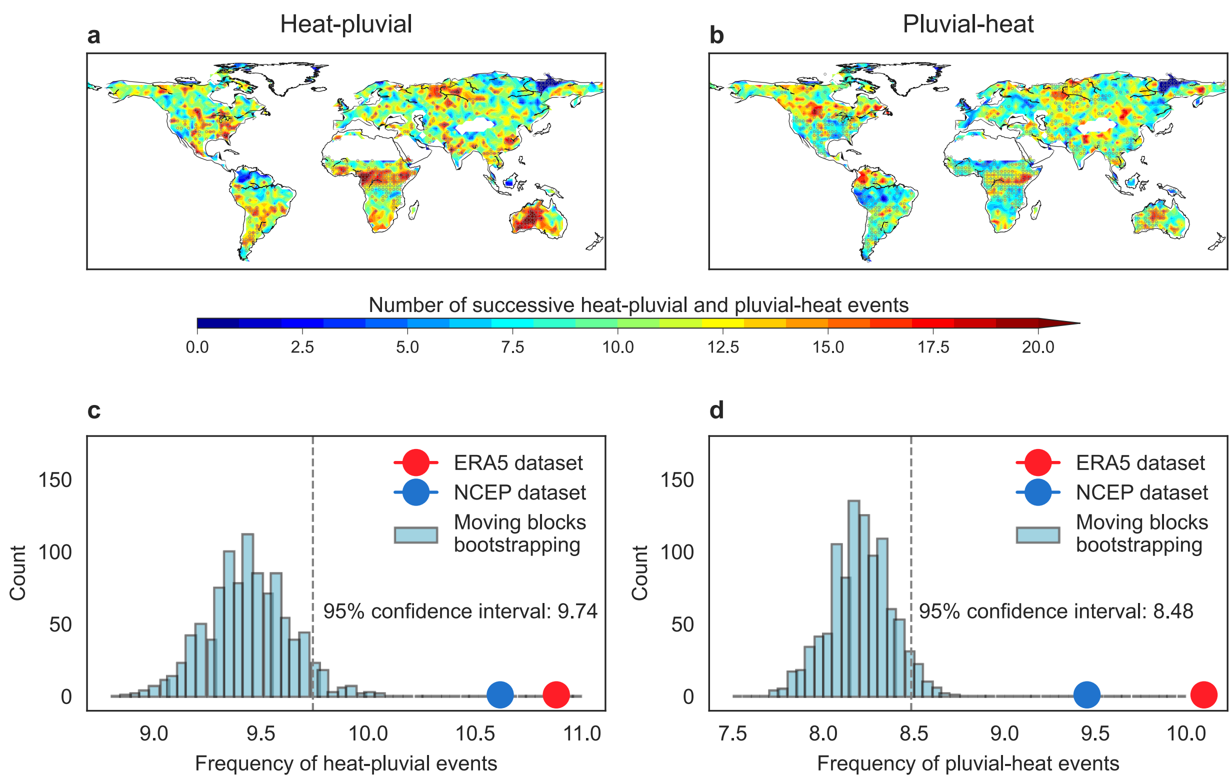

Figure 1. Frequency of successive heat-pluvial and pluvial-heat events within 7 days during 1956–2015. a, b Spatial maps showing the total number of successive heat-pluvial and pluvial-heat events, respectively. Grid cells that are statistically significant at the 0.05 level according to the moving-blocks bootstrap-resampling-based test are depicted as grey circles. The dataset used here is ERA5. **c, d** Significance test of the global-mean consecutive occurrence frequencies using moving-blocks bootstrap resampling based on ERA5 dataset for the heat-pluvial events (**c**) and pluvial heat events (**d**), respectively. The histogram represents the empirical distribution of successive events frequency using the 1,000 resampled series based on the moving-blocks bootstrap resampling. The 95% confidence interval is indicated by a vertical dashed line. The red dot and blue dot represent the number of successive events detected based on ERA5 and NCEP datasets, respectively.

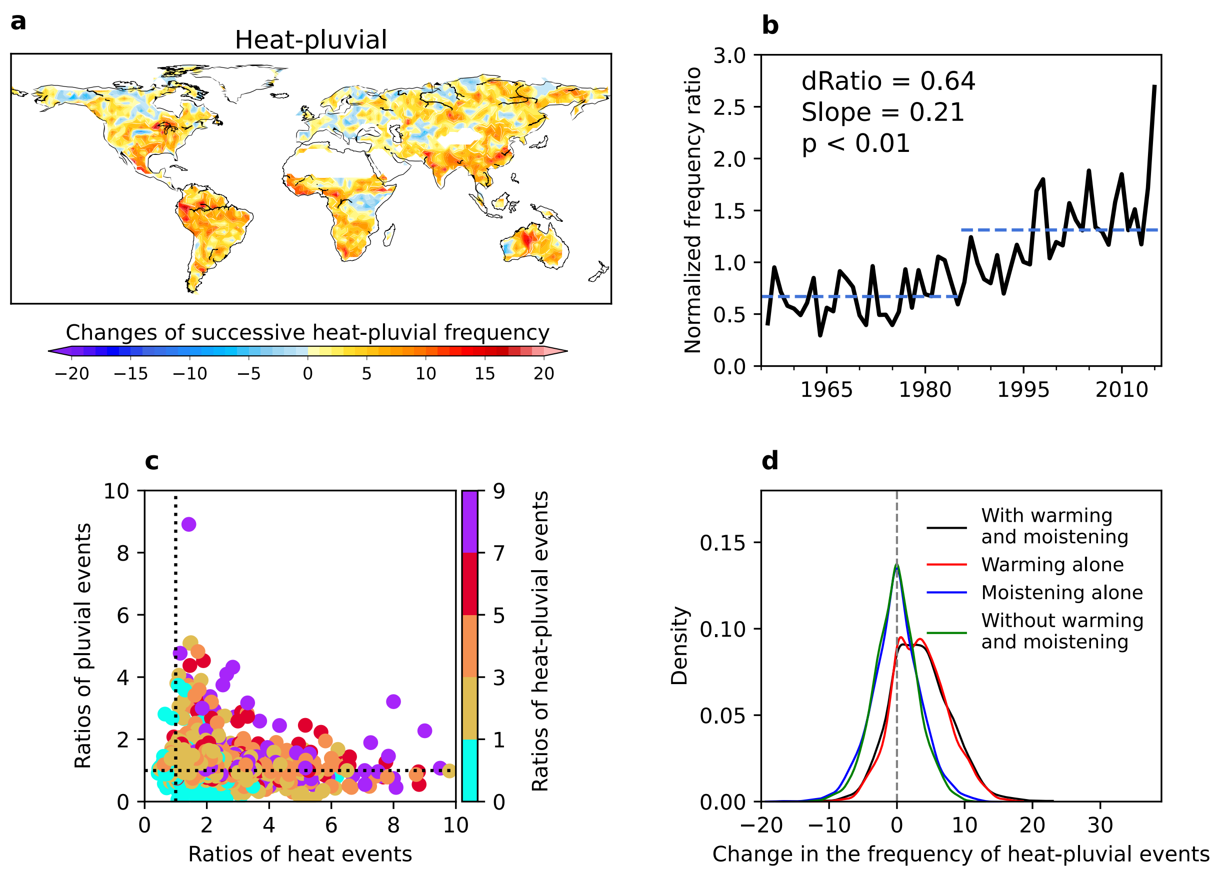

Figure 2. Spatiotemporal changes and decomposition in the frequency of successive heat-pluvial events within 7 days. a Spatial change in successive heat-pluvial events between the two 30-year periods (recent, 1986–2015 minus past, 1956–1985). **b** Annual time series of the normalized frequency ratio of successive heat-pluvial events. Black line is the annual normalized frequency ratio based on ERA5; blue dashed line is the 30-year average. dRatio is the difference between the averages during 1956–1985 and 1986–2015; Slope is the linear trend using the Sen-slope method (unit, decade-1). **c** The relationship between the changes in successive events and changes in individual extremes. Color circles show bin-averaged ratios of heat-pluvial events corresponding to ratios of individual extremes. **d** Decomposition of the frequency of heat-pluvial events due to warming/moistening effects. It shows the probability density function of the global mean changes in the frequency of heat-pluvial events between the two 30-year periods, based on

raw observational data (black), data with moistening signal removed (red), data with warming signal removed (blue) and data with both warming and moistening signals removed (green).

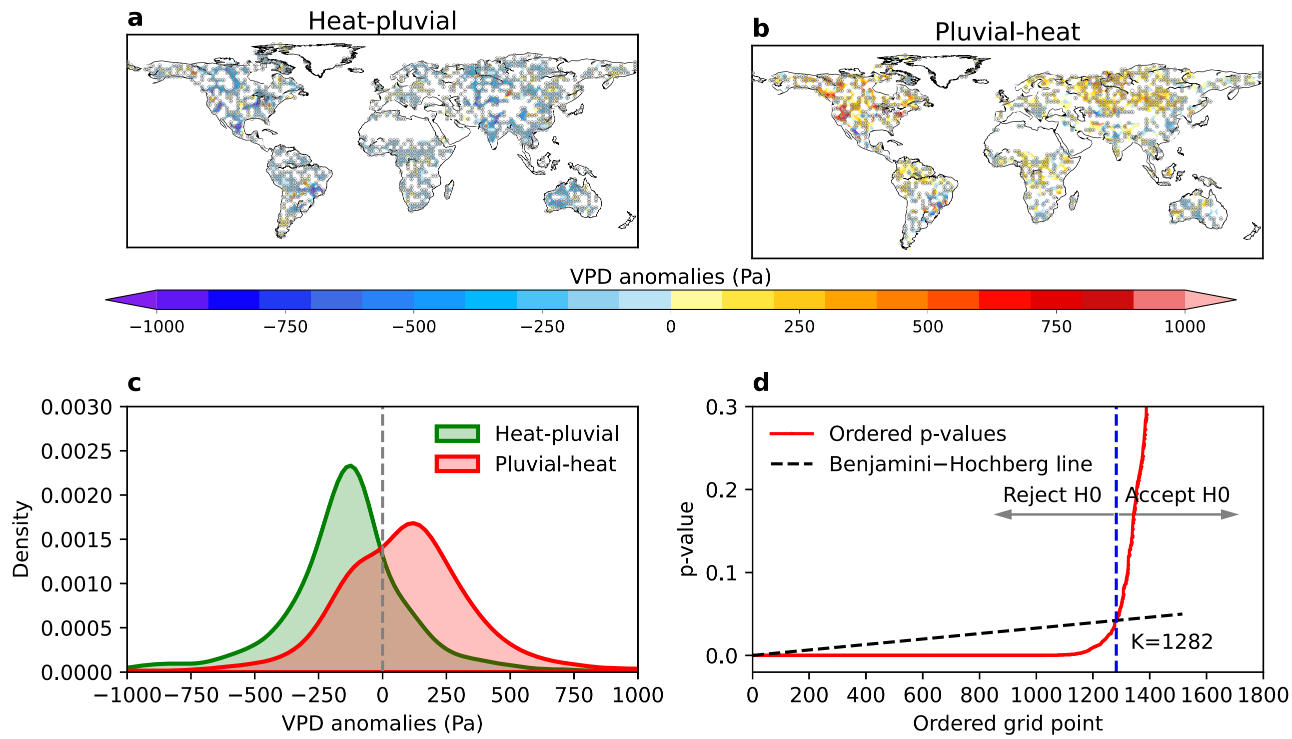

Figure 3. The behavior of VPD anomalies in the transition between heat and pluvial events. **a** represents VPD anomalies between heat events followed by pluvial events (heat-pluvial) and heat events not followed by pluvial events (heat-without-pluvial). **b** represents VPD anomalies between pluvial events followed by heat events (pluvial-heat) and pluvial events not followed by heat events (pluvial-without-heat). Grid points that satisfy local statistical significance at the 0.05 level are shown as grey circles, while the ones that meet the FDR criterion by having a sufficiently small p-value are marked by grey points. **c** is the probability density function of the map **a** (green line) and **b** (red line) for the VPD anomalies causing the transition between heat and pluvial events. **d** is the FDR for testing field significance of VPD anomalies (Pa) between heat-pluvial and heat-without-pluvial events.